

GLASS-CERAMIC SYSTEMS COMPATIBLE WITH THE FIRING CONDITIONS USED IN THE CERAMIC TILE INDUSTRY

Eduardo Quinteiro^(*), Anselmo Ortega Boschi^(**),

Cristina Leonelli^(***), Tiziano Manfredini^(***), Cristina Siligardi^(***)

^(*)Centro Cerâmico do Brasil, e-mail: quinteiro@ccb.org.br, São Paulo, Brasil

^(**)Universidade Federal de São Carlos – Laboratório de Revestimentos Cerâmicos,
São Carlos, Brasil.

^(***)Università degli Studi di Modena e Reggio Emilia, Modena, Italia

ABSTRACT

Glass-ceramic materials possess an enormous potential for use in glazes for ceramic tiles. However a devitrification process needs to take place for ceramic frits during the fast single-fire cycles typically used in processing glazed floor tiles. Thus, such frits should have a well-selected and controlled chemical composition, so that the kinetic crystallisation process, during fast firing, will take place intensely, producing a glaze with a high crystalline fraction. Besides crystallisation during firing, glaze densification should also occur in such a way as to yield a compact layer, practically free of porosity. Unfortunately, sintering and crystallisation of the reacting milled frit powders do not occur in different temperature ranges during thermal treatment in a single cycle. These two kinetic processes usually develop simultaneously in the same temperature range, causing mutual interference. The objective of this study was first to identify and to evaluate glass-ceramic systems that devitrify during fast single-fire cycles and, subsequently, to establish common ground between them with regard to the correlations between crystallisation and densification. The eight studied systems were found to be suitable for developing significant proportions of crystalline phases in the heat treatment process with high heating and cooling rates. A systematic relationship between crystallisation and densification can be observed on using differential thermal analysis and hot stage microscopy techniques for the combined analysis of this behaviour.

INTRODUCTION

Glass-ceramic materials are polycrystalline solids that contain a residual glassy phase. They are prepared based on controlled crystallisation of molten glasses. The interest in these materials is fundamentally due to their singular characteristics compared with glass and ceramic materials ^[1].

Glasses, on initially having a larger energy content than that corresponding to their thermodynamic balance, can crystallise in favourable conditions. This process is known as devitrification, in which crystal nucleation and growth are the predominating mechanisms ^[2].

All the characteristics indicate that glass-ceramic materials are quite appropriate for glazes, since they develop the desired technical characteristics during processing, producing a layer free of defects and with better resistance to mechanical stresses.

On the other hand, design of a glass-ceramic glaze for floor tiles should ensure that the selected frit precursor is technically and commercially compatible with the manufacturing conditions generally used in the production of glazed ceramic floor tiles. Thus, the preparation of devitrifiable frits used as one of the major components in floor tile glazes, need to satisfy certain requirements regarding their devitrification and sintering behaviour, besides being compatible with the characteristics of the engobe and body.

Glazes are consolidated by sintering milled frits (glassy powders of high specific surface area) in a single thermal treatment. Their densification is achieved by means of sintering in the presence of a viscous flow that arises at slightly higher temperatures than the glass transition temperature (T_G). Thus, above T_G , viscosity tends to decrease and each glassy particle tends to become spherical. Liquid phase forms between the particles and if the temperature is sufficiently high to maintain certain degree of viscosity, these will begin to form a structural connection by necking ^[3].

The literature describes the obtainment of glass-ceramic materials by long nucleation and growth programs ^[1,4], most of the known systems being incompatible with fast-single fire cycles. Besides this, for producing glass-ceramic glazes in a fast cycle, densification of the glaze layer needs to be completed at a lower temperature than that of crystallisation start, thus producing dense materials of low porosity, which are at the same time well crystallised. However, this ideal sequence of events does not always develop, because the crystallisation phase can occur before or simultaneously with sintering ^[3].

EXPERIMENTAL PROCEDURE

MATERIALS

Eight frits were selected, based on previous studies, which showed that such compositions presented kinetic crystallisation behaviour compatible with fast single-fire cycles. The glassy systems used were referenced as follows: *MAS*, *ZnLAS*, *ZrLS*, *ZrKCS*, *ZnAS*, *CBAS*, *ZrCMS* and *CMAS*. The chemical compositions of these frits are shown in Table 1.

The melting batches containing the raw materials were homogenised by dry milling in a rotary ball mill for 5min. The compositions were placed in crucibles of ZAS

(zirconium-alumina-silica) for melting. A laboratory melting kiln was used at a heating rate of 5°C/min to a temperature of 1000°C, holding this temperature for 15min, which was enough time to complete the decomposition reactions of the carbonate precursors. The temperature was raised to 1500°C with a rate of 10°C/min. After 20 minutes, the material was quenched in water, and the resulting frits were separated and dried in an oven.

CHARACTERISATION OF DEVITRIFICATION BEHAVIOUR

Each frit was prepared in the laboratory and wet milled in a rotary mill. Mill time was varied so that no reject was obtained on a screen with 44µm mesh aperture. The resulting dry powders were moistened with 7% water by weight and unidirectionally pressed at 250kgf/cm², forming cylindrical disks with a 3.5cm diameter and mass of approximately 10g. These test specimens were subjected to different thermal treatments, varying peak firing temperature (Table 2). The heating and cooling rate used was 20°C/min, with a 5min hold at peak firing temperature.

The sintered pieces were milled until reaching a particle size below 44µm and analysed with regard to the devitrified crystalline phases by X-ray diffraction (XRD) (powder method). A *Philips PW3710* diffractometer was used, with a copper tube, scanning in the range (2θ) from 10° to 60°, at a rate of 1°/min.

Samples of each frit, with particle size below 44µm, were subjected to heating tests by differential thermal analysis (DTA), with a *Netzsch, STA 409* instrument. A heating rate of 20°C/min was used, determining the glass transition temperature (T_C), crystallisation temperature (T_C) and melting temperature (T_F). The same test was carried out in the samples that contained particles of sizes between 177µm and 297µm. Shifts in the crystallisation peak for the different particle sizes indicated the predominance of a surface crystallisation process ^[5].

The microstructures obtained after the different thermal treatments (Table 2) were observed by scanning electron microscopy (SEM).

Oxide	Oxide wt%							
	MAS	ZnLAS	ZrLS	ZrKCS	ZnAS	CBAS	ZrCMS	CMAS
SiO ₂	53,00	60,96	63,33	51,70	40,00	37,42	45,00	47,80
Al ₂ O ₃	30,00	10,01	—	—	20,00	6,52	—	22,2
MgO	17,00	6,6	—	—	—	—	22,50	7,6
TiO ₂	—	6,54	—	—	—	0,50	—	—
ZnO	—	11,98	—	—	30,00	—	—	—
Li ₂ O	—	3,91	13,50	—	—	—	—	—
ZrO ₂	—	—	23,17	11,28	—	0,50	10,00	—
K ₂ O	—	—	—	6,00	—	—	—	—
CaO	—	—	—	31,02	—	17,46	22,50	22,4
B ₂ O ₃	—	—	—	—	10,00	—	—	—
BaO	—	—	—	—	—	37,60	—	—

Table 1: Chemical compositions of the frits used in the study.

	Temperatures (°C)
<i>MAS</i>	950, 1000, 1050, 1100 y 1150
<i>ZnLAS</i>	1000, 1050, 1100, 1150 y 1200
<i>ZrLS</i>	750, 800, 850, 900, 950, 1000
<i>ZrKCS</i>	1000, 1050, 1100, 1150 y 1200
<i>ZnAS</i>	950, 1000, 1050, 1100 y 1150
<i>CBAS</i>	850, 900, 950, 1000 y 1050
<i>ZrCMS</i>	850, 900, 950, 1000 y 1050
<i>CMAS</i>	850, 900, 950, 1000 y 1050

Table 2: Maximum heat-treatment temperatures (heating and cooling rates of 20°C/min and 5min hold at peak temperature).

CHARACTERISATION OF SINTERING BEHAVIOUR

In the milled frit samples, with particles smaller than 44µm, diagrams were obtained that correlate the decrease in height of pressed cylindrical specimens (2mm diameter and 2mm height) with the increase in temperature, based on images in black and white produced by hot stage microscopy. During the test the specimens were set on a sintered alumina base. Images of the sample profiles were recorded in 10°C steps during heating at 20°C/min. The densification start temperature (T_D) and softening start temperature (T_A) were determined of each frit.

VICKERS MICROHARDNESS AND MICROSTRUCTURE

The determination of hardness according to the Mohs scale does not represent an accurate measure for evaluating ceramic materials, due to the subjectivity in the evaluation of the results. More significant evaluations with this property can be found in ceramic surfaces by determining Vickers microhardness [6]. The highest values for this characteristic in ceramic glazes indicate better performance with regard to risks and abrasion resistance [7].

The specimens sintered at 1150°C of the devitrifiable frits were prepared by embedding in resin. The test surfaces were previously subject to abrasion and polishing. The apparatus used to measure Vickers microhardness was a *Digital Microhardness Tester FM* made by the *Future Tech Corporation*. At least five measurements were made per sample applying variable loads (P) (100g, 200g and 500g) for 10 seconds. Subsequently, the diagonals of the indent were measured (l) and the microhardness values (Hv) calculated by means of Equation 1.

$$H_v = \frac{1.854 P}{l^2} \tag{1}$$

RESULTS AND DISCUSSION

Table 3 sets out the main data on the crystalline phases identified in the X-ray diffractograms for the frits that were milled and subjected to different thermal treatments (Table 2). All the compacts, at a temperature of 1000°C, presented a significant presence of crystalline phases of interest in the glazes for ceramic floor tiles. The results of the XRD analysis are discussed below.

MAS. The crystallisation of glasses in this system is known to be a complex process, due to the great number of phases, many of them metastable, which can crystallise from the precursor glass [5]. It was observed that Indialite, one of the structural forms of Cordierite, exhibited growing diffracted peak intensity with increasing maximum heat-treatment temperature, indicating the main phase starting at 1000°C.

ZnLAS. β -spodumene (Aluminium-Lithium Silicate) appears as the main phase in the diffractograms of the samples treated at different temperatures, mainly at 1050°C and 1100°C. It is known that when the TiO_2 is used as a nucleating agent, the development of Rutile accompanies the transformation of the β -spodumene phase [8].

ZrLS. The Lithium Silicates are the main phases that form by thermal treatments up to a temperature of 950°C. In the samples treated at 1000°C, Zirconium Silicate is the major phase present [9].

ZrKCS. Wollastonite was the main crystallising phase, presenting peaks of practically unaltered intensity for thermal treatments from 1000°C up to 1150°C, while this phase was not detected at 1200°C. At this last temperature, the Zirconium and Calcium-Zirconium Silicates were the main phases present in the samples [10].

	Oxides Present	Crystalline Phases Formed				
		Name	General Composition	JPCDS file	System	Density
MAS	SiO_2 , Al_2O_3 , MgO	Indialite, <i>syn</i>	$\alpha\text{-Mg}_2\text{Al}_4\text{Si}_5\text{O}_{18}$	13-0293	hexagonal	2.51
		Al-Mg Silicates	$(\text{Mg},\text{Al})\text{SiO}_3$	35-0310	orthorhombic	3.28
			$\text{MgAl}_2\text{Si}_2\text{O}_{10}$	25-0511	hexagonal	2.57
ZnLAS	SiO_2 , Al_2O_3 , MgO, TiO_2 , ZnO, Li_2O	Li-Al Silicate	$\text{LiAlSi}_3\text{O}_8$	35-0794	tetragonal	3.20
		Willemite, <i>syn</i>	Zn_2SiO_4	37-1485	rhombohedral	4.25
		Rutile, <i>syn</i>	TiO_2	21-1276	tetragonal	4.25
		Enstatite	MgSiO_3	22-0714	orthorhombic	3.19
		Quadilite, <i>syn</i>	Mg_2TiO_4	25-1157	cubic	3.55
ZrLS	SiO_2 , Li_2O , ZrO_2	Zr Silicate	ZrSiO_4	06-0266	tetragonal	4.67
		Li Silicates	Li_2SiO_3	29-0829	orthorhombic	2.53
			$\text{Li}_2\text{Si}_2\text{O}_5$	40-0376	monoclinic	2.46
		Baddeleyite, <i>syn</i>	ZrO_2	37-1484	monoclinic	5.82
		Moganite	SiO_2	38-0360	monoclinic	2.64
		Stishovite	SiO_2	15-0026	tetragonal	4.29
ZrKCS	SiO_2 , ZrO_2 , K_2O , CaO	Baghdadite, <i>syn</i>	$\text{Ca}_3\text{Zr}(\text{Si}_2\text{O}_7)_2$	39-0195	monoclinic	3.80
		Wadleyite, <i>syn</i>	$\text{K}_2\text{ZrSi}_3\text{O}_9$	35-0031	hexagonal	3.11
		Silicate Zr	ZrSiO_4	33-1485	tetragonal	5.25
		Wollastonite, 2M	CaSiO_3	27-0088	monoclinic	2.91
ZnAS	SiO_2 , Al_2O_3 , ZnO, B_2O_3	Gahnite, <i>syn</i>	ZnAl_2O_4	05-0669	cubic	4.61
		Willemite, <i>syn</i>	Zn_2SiO_4	37-1485	rhombohedral	4.25
CBAS	SiO_2 , Al_2O_3 , TiO_2 , ZrO_2 , CaO, BaO	Celsian, <i>syn</i>	$\text{BaAl}_2\text{Si}_2\text{O}_8$	38-1450	monoclinic	3.39
		Al-Ba Silicate	$\alpha\text{-BaAl}_2\text{Si}_2\text{O}_8$	12-0725	orthorhombic	3.30
		Ba-Zr Silicate	$\text{Ba}_2\text{Zr}_2\text{Si}_2\text{O}_{12}$	19-0148	—	—
		Walstromite	$\text{BaCa}_2\text{Si}_3\text{O}_9$	18-0162	triclinic	3.73
ZrCMS	SiO_2 , MgO, ZrO_2 , CaO	Diopside	$\text{CaMg}(\text{SiO}_3)_2$	11-0654	monoclinic	3.26
		Forsterite, <i>syn</i>	Mg_2SiO_4	34-0189	orthorhombic	3.22
		Baddeleyite, <i>syn</i>	ZrO_2	36-0420	monoclinic	5.82
		Akermanite, <i>syn</i>	$\text{Ca}_2\text{MgSi}_2\text{O}_7$	35-0592	tetragonal	2.95
CMAS	SiO_2 , Al_2O_3 , MgO, CaO	Diopside, <i>aluminian</i>	$\text{Ca}(\text{Mg},\text{Al})(\text{Si},\text{Al})_2\text{O}_6$	41-1370	monoclinic	3.29
		Anorthite	$\text{CaAl}_2\text{Si}_2\text{O}_8$	41-1486	triclinic	2.76

Table 3: Phases identified in the X-ray diffractograms of the heat treated frits.

ZnAS. Gahnite was the major identified phase at all the test peak heat treatment temperatures. The largest presence of Willemite was mainly observed at 1050°C [11].

CBAS. At temperatures of 850°C and 900°C, diffracted peaks were not observed, hardly evidencing amorphous bands. With the three highest temperatures (950°C, 1000°C and 1050°C), the nature and intensity of the phase peaks remained practically unaltered. Barium-Aluminium Silicates are the major phases that form ^[12].

ZrCMS. At 850°C, Forsterite is the main crystallised phase. At temperatures of 900°C or higher, Diopside becomes the main phase, while the peak intensities of the initially formed Forsterite practically stay constant. The study of the effect of the use of different nucleating agents on crystallisation in this system, shows that ZrO₂ yields crystals of 1 to 5µm, while TiO₂ produces crystals smaller than 0.5µm ^[13].

CMAS. Significant crystallisations were not detected with treatment at a maximum temperature of 850°C. At the other temperatures, the main phases that formed were Diopside and Anorthite ^[14].

For the eight systems, the resulting microstructures exhibit crystals that do not usually exceed 10µm. These crystals, are sufficiently numerous and interact with each other, not being simply dispersed in a glassy matrix. Figure 1 shows some of microstructures found.

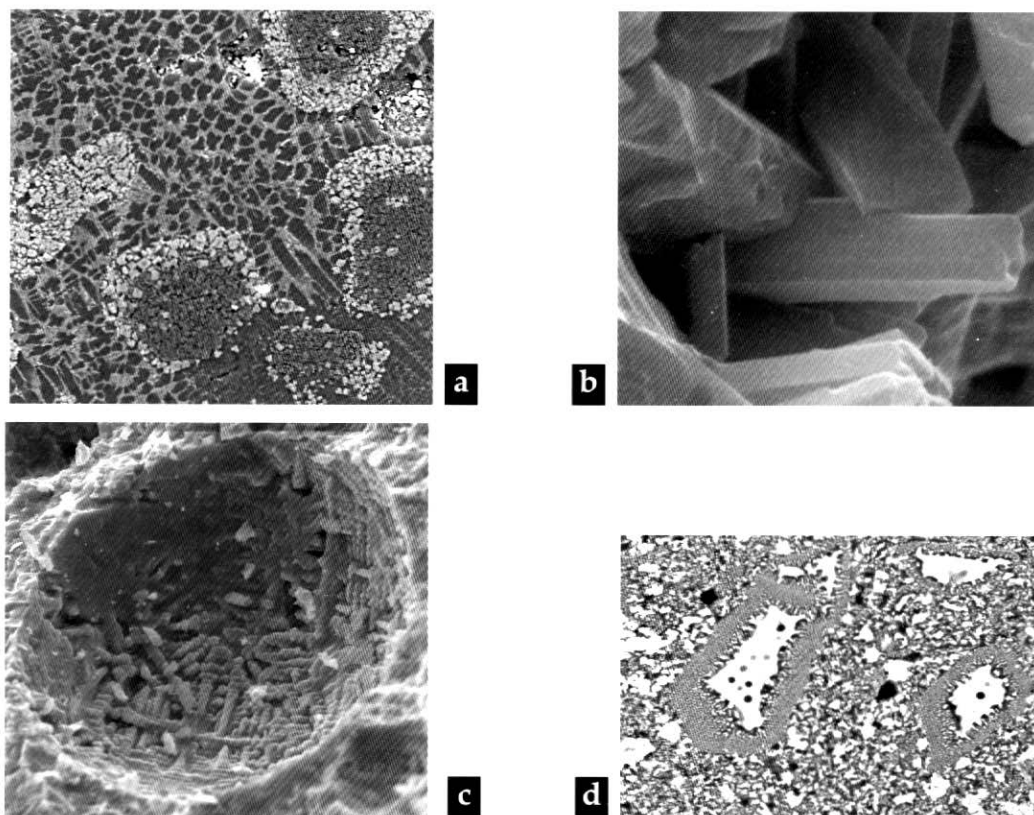


Figure 1: (a) polished surface of ZnLAS treated at 1150°C; (b) fracture surface of ZrLS: treated at 950°C; (c) isolated pore in ZnLAS treated at 1150°C; (d) polished surface of ZnAS treated at 1050°C.

The thermograms found by DTA (characteristic values in Table 4) show:

- Initially, with the increase in temperature not very pronounced endothermic events occur, corresponding to an increase in specific heat, which means glass transition (T_G);

- Exothermic events, at higher temperatures than transition temperatures, indicating crystallisation temperatures (T_C);
- Endothermic events, at still higher temperatures, indicating melting of the crystalline phases (T_F).

The values of densification start temperature (T_I) and softening start temperature, found in the hot stage microscopy test, are also given in Table 4. Densification start (T_I) occurs consistently at a higher temperature than T_C for all the frits.

	Temperature (°C)							
	Differential Thermal Analysis						Hot Stage Microscopy	
	T_G	T_{C1}	T_{C2}	T_{C3}	T_{F1}	T_{F2}	T_I	T_A
<i>MAS</i>	781	950	1007	1113	1317	—	890	1440
<i>ZnLAS</i>	592	786	—	—	1132	—	700	1140
<i>ZrLS</i>	562	785	900	954	938	976	640	990
<i>ZrKCS</i>	770	1017	—	—	1230	1282	830	1331
<i>ZnAS</i>	654	879	—	—	—	—	750	—
<i>CBAS</i>	717	1011	—	—	1221	—	790	1229
<i>ZrCMS</i>	722	940	—	—	1300	—	790	1301
<i>CMAS</i>	753	919	—	—	1249	—	840	1290

Table 4: Value measured by differential thermal analysis: glass transition temperature (T_G), crystallisation temperature (T_{C1} , T_{C2} and T_{C3}), melting temperature (T_{F1} , T_{F2} and T_{F3}). Values measured by hot stage microscopy: densification start temperature (T_I) and softening temperature (T_A).

A temperature shift was observed in the most intense crystallisation peak, when samples that contained different particle size ranges were subjected to differential thermal analysis. The crystallisation temperatures (T_C) obtained in the samples with the coarsest particles (between 177 and 297 μ m) were found to be higher than the temperatures corresponding to crystallisation of the samples containing the finer particles (smaller than 44 μ m), indicating the predominance of a surface nucleation process. The differences in crystallisation temperatures (ΔT_C) are shown in Table 5. As crystallisation in these systems developed preferentially from the frit particle surface, variations in the specific surfaces found in the glaze milling process can also be involved in the changes of the number and size of the crystals, and can hence cause alterations in the visual appearance of the glazed floor tile surface. The micrographs in Figures 1(c) and 1(d) respectively show the preferential nucleation of Zirconium Silicate at the surface of an isolated pore in *ZnLAS* and surface nucleation of Gahnite in *ZnAS*.

	Frit							
	<i>MAS</i>	<i>ZnLAS</i>	<i>ZrLS</i>	<i>ZrKCS</i>	<i>ZnAS</i>	<i>CBAS</i>	<i>ZrCMS</i>	<i>CMAS</i>
ΔT_C (°C)	43,3	42,8	53,3	53,3	66,5	55,5	58,1	84,5

Table 5: Differences in temperature of the main characteristic crystallisation peaks of frit samples with coarse particles (between 177 and 297 μ m) and fine particles (smaller than 44 μ m).

Figure 2 shows the values of specimen dimensional variation, obtained in the hot stage microscope, correlating the percentage of initial height with the increase in temperature. Together with each one of these plots, the respective DTA of the frit is shown, to facilitate a correlation between crystallisation and sintering. Common

behaviour was observed in all the frits in Figure 2, where at a higher temperature to that of sintering start (T_i), a flattening always occurs in the curves, there not being any increase in shrinkage, before the softening temperature is reached (T_A). It is important to note that the beginning of this flattening coincides with the temperature at which the first crystallisation occurs for each frit (T_{C1}). This demonstrates that crystal formation plays a decisive role in the change of sintering behaviour in an initially glassy system.

During heating, the densification of the specimens that began at T_i is interrupted when the first crystallisation arises at temperature T_{C1} . Starting from this temperature, the shrinkage of the specimens ceases. Thus, at a temperature of T_{C1} , there is probably an alteration in the sintering mechanism of the system. In this case, the predominant densification mechanism would go together with a diffusion process by viscous flow to solid state diffusion, because the crystals are fundamentally formed on the surface of the particles, this being the region initially occupied by the viscous phase. Solid state sintering could occur on contributing enough energy and time to the system, this not being possible given the high heating rate used. In the eight studied systems of Figure 2, the frits reinitiate densification at temperatures close to melting temperatures (T_F) of at least one of the crystalline phases, when a liquid phase reappears and the initial densification mechanism predominates again.

Frit *ZnAS* presented different behaviour (Figure 2), its densification reinitiating after the first crystallisation (T_{C1}) just before melting of the crystalline phases formed (Gahnite and Willemite were found as stable phases, in the X-ray diffractograms in the range between 950° and 1150°C). This behaviour is probably due to the presence of Boron Oxide in its formula, working as a vigorous flux at temperatures below 1000°C.

After observing the correlation between crystallisation and densification, it would be important to have a low rate of surface crystallisation for the sintering of the glass-ceramic systems [3]; however, this becomes a negligible problem when such high heating and cooling rates are used.

As expected, the Vickers microhardness results (Table 6) show that in the specimens treated thermally at 1150°C, crystallisations occur in those with the greatest hardness, on comparing these with specimens made with frits in which significant devitrifications do not occur (frits *Commercial-A* and *Commercial-B*).

Exceptionally there is *CBAS* that presented a microhardness comparable to those of the specimens made with frit *Commercial-A*. The relatively low microhardness values and the high mean STD deviation found for sample *ZrLS* seem to be related to the presence of a large fraction of small pores in the specimens processed in this condition. Sample *ZnLAS* exhibited ranges of very different microhardness values depending on where the indent was made. The microstructure of this sample was quite heterogeneous (Figure 1(a)), exhibiting different regions that could individually exceed the dimensions of the indents.

Frit	Vickers Microhardness (10 ² Kg/mm ²)
<i>MAS</i>	9,9 ± 0,7
<i>ZnLAS</i>	8 ± 1
	14 ± 1
<i>ZrLS</i>	7 ± 1
<i>ZrKCS</i>	7,2 ± 0,5
<i>ZnAS</i>	8,3 ± 0,7
<i>CBAS</i>	5,6 ± 0,3
<i>ZrCMS</i>	8,6 ± 0,1
<i>CMAS</i>	9,0 ± 0,7
<i>Commercial A</i>	5,4 ± 0,5
<i>Commercial B</i>	5,8 ± 0,3

Table 6: Vickers microhardness of frit compacts sintered at 1150°C.

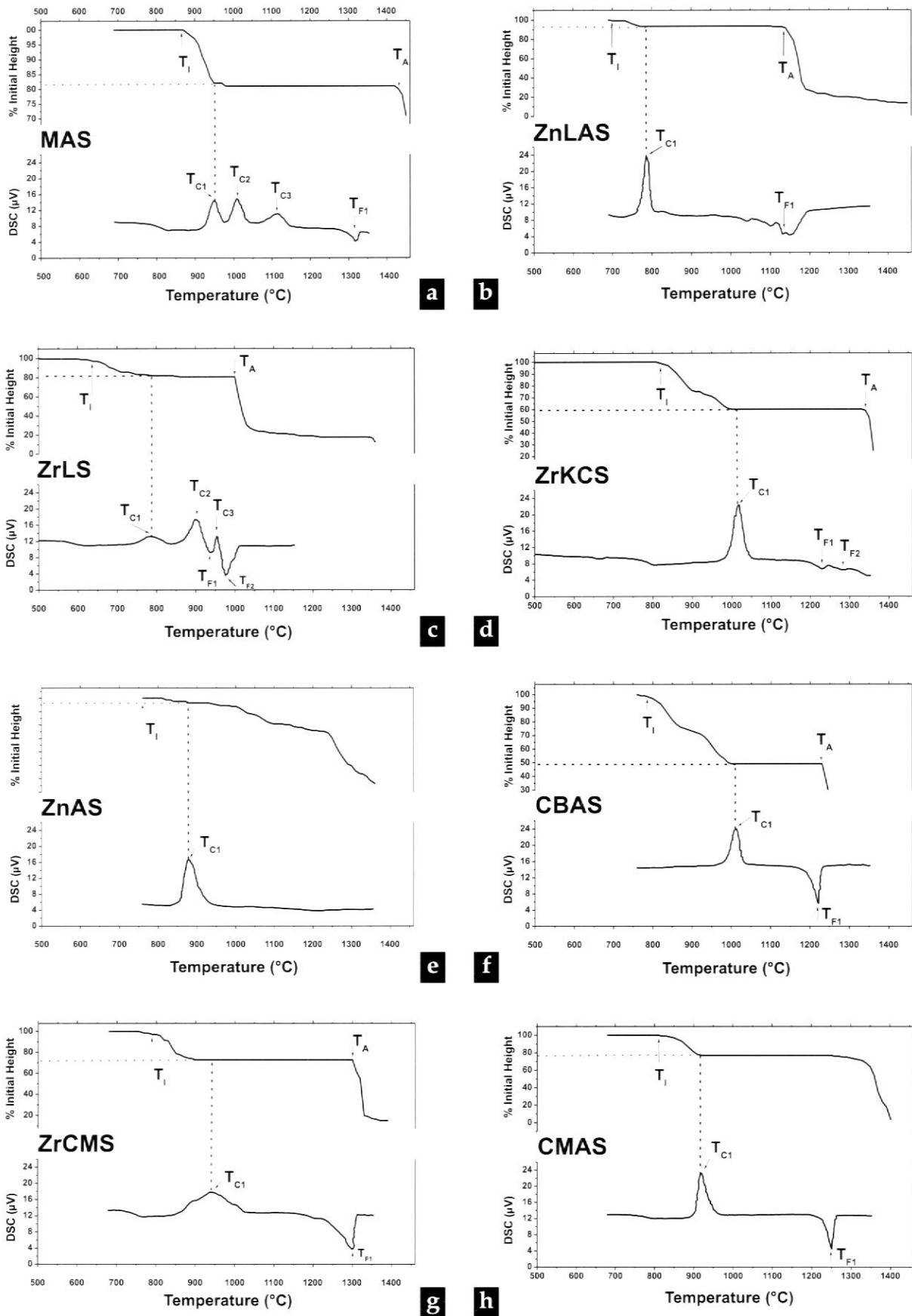


Figure 2: Sintering behaviour (hot stage microscopy and crystallisation (DTA)).

CONCLUSIONS

The most significant conclusions to be drawn from the experiments carried out with the devitrifiable frits (*MAS, ZnLAS, ZrLS, ZrKCS, ZnAS, CBAS, ZrCMS, CMAS*) are:

- With regard to devitrification behaviour, in all the studied frits the presence of surface crystallisation predominated.

- With the thermal treatments used, all the compacts prepared with the milled frits presented a significant presence of crystalline phases of interest in glazes for floor tiles at a temperature of 1000°C.

- The microstructures produced present crystals that do not usually exceed 10µm. These crystals appear, in all the cases, in sufficiently numerous quantities and interact with each other, not being simply dispersed in the glassy matrix.

- To understand the correlation between devitrification and sintering it is especially important to foresee the effect of using frits of this nature in designing glaze surfaces. Combined analysis of the results of the hot stage microscopy and differential thermal analysis techniques enable making certain observations:

- Densification starts at temperature T_V , which exceeds the glass transition temperature (T_G).
- The systems maintain a high densification rate up to the temperature at which crystallisation of the first crystalline phase occurs (T_{C1}).
- At temperatures just above those of first phase crystallisation (T_{C1}), there is no significant rise in densification.
- Densification takes place again when viscous flow reappears, or after a softening temperature (T_A) when melting of at least one crystalline phase at T_{F1} has already occurred, or when a vigorous flux is present in its formula (as in the case of B_2O_3 in the *ZnAS* formula).

- Thermal treatments at 1150°C produced specimens with higher microhardness, compared with the results for commercial non-devitrifiable frits processed under the same conditions, owing to the properties of the crystals present and the resulting microstructures.

REFERENCES

- [1] BARBIERI, L.; LEONELLI, C.; MANFREDINI, T. Technological and product requirements for fast firing glass-ceramic glazes. **Ceramic Engineering and Science Proceedings**, v. 17, n. 1, p. 11-22, 1996.
- [2] NAVARRO, J.M.F. **El vidrio: constitución, fabricación, propiedades**. Madrid: Consejo Superior de Investigaciones Científicas / Instituto de Cerámica y Vidrio, 1985. 667p.
- [3] SILIGARDI, C.; D'ARRIGO, C.; LEONELLI, C. Sintering behavior of glass-ceramic frits. **American Ceramic Society Bulletin**, v.79, n. 9, p. 88-92, 2000.
- [4] MANFREDINI, T.; PELLACANI, G. C.; RINCON, J. M. **Glass-ceramic materials, fundamentals and applications**. Modena: Mucchi Editore, 1997. 250p.
- [5] FERRARI, A.M. et al. Feasibility of using cordierite glass-ceramics as tile glazes. **Journal of the American Ceramic Society**, v. 80, n. 7, p. 1757-1766, 1997.
- [6] BIFFI, G. **Abrasione**. Faenza: Faenza Editrice, 1992. 123p.

- [7] ESPOSITO, L. et al. Vickers indentation method applied to the characterization of ceramic glazes. **Ceramic Engineering and Science Proceedings**, v. 15, n. 1, p. 146-159, 1994.
- [8] BEALL, G. H. Design of glass-ceramics. **Reviews of Solid State Science**, v. 3, n. 3/4, p. 113-134, 1989.
- [9] ESCARDINO, A. et al. Estudio de la formación de fases cristalinas en vidriados blancos de zirconio. En: CONGRESO MUNDIAL DE LA CALIDAD DEL AZULEJO Y DEL PAVIMENTO CERÁMICO, 1996, Castellón/España. **Actas**. Castellón: 1996. p. 173-189.
- [10] BALDI, G. et al. Vetroceramici appartenenti al sistema $\text{CaO-SiO}_2\text{-ZrO}_2$ come componenti di smalti per piastrelle. **Ceramurgia**, v. 8, p. 139-142, 1995.
- [11] ESCARDINO, A. et al. Crystallization in $\text{SiO}_2\text{-Al}_2\text{O}_3\text{-ZnO-TiO}_2$ glass: process mechanism. **British Ceramic Transactions**, v. 98, n. 4, p. 196-199, 1999.
- [12] BARBIERI, L. et al. The microstructure and mechanical properties of sintered celsian and strontium-celsian glass-ceramics. **Materials Research Bulletin**, v. 30, n. 1, p. 27-41, 1995.
- [13] BALDI, G. et al. Effects of nucleating agents on diopside crystallization in new glass-ceramics for tile-glaze application **Journal of Material Science**, v. 30, p. 3251-3255, 1995.
- [14] LEONELLI, C. et al. Crystallization of some anorthite-diopside glass precursors. **Journal of Materials Science**, v. 26, p. 5041-5046, 1991.

ACKNOWLEDGEMENTS

The authors express their gratitude to the FAPESP (process 97/02254-5) for the resources provided for the performance this study.